Applied Machine Learning-Based Metal Additive Manufacturing for Lightweight Aerospace Components

Austin Prevette[1] Kimberton Mai[2] Spencer Garrett[3] Neil Sanipara[4]
Mississippi State University, Mississippi State, MS, 39762

Metal additive manufacturing (AM) is an emerging paradigm in aerospace design; AM enables fabrication of structures that are impractical through traditional manufacturing methods. Additionally, these additive designs can utilize self-supporting Topology Optimization (TO) to drastically increase specific yield and specific 1st mode. The resulting mass-efficient designs reduce failure stress by up to three times compared to their subtractive counterparts. These AM and AM+TO designs are optimized using Kriging-based engineering surrogate modeling techniques and the resulting novel components are rigorously tested against various criteria—including yield failure testing, random vibration testing, and real-world flight tests. This paper validates the compressive strength and vibrational response of these parts at Mississippi State University's Advanced Composites Institute and NASA MSFC, respectively. Based on the results of the validation tests, the AM components exceed specified testing criteria and will thus be flown on a high-powered rocket for IREC 2025, pioneering technology in applied student aerospace engineering.

I. Nomenclature

ACI	=	Advanced Composites Institute
AM	=	Additive Manufacturing
ASD	=	Acceleration Spectral Density
BC	=	Boundary Condition(s)
CAVS	=	Center for Advanced Vehicular Systems
DFAM	=	Design for Additive Manufacturing
F.S.	=	Factors of Safety
GEVS	=	General Environmental Verification Standard
GSTOR	=	Generative STructural Optimization Routine
HAC	=	Hybrid Avionics Coupler
HPCC	=	High-Performance Computing Collaboratory
IC	=	Initial Condition(s)
ML	=	Machine Learning
MSFC	=	Marshall Space Flight Center
RLH	=	Random Latin Hypercube
TO	=	Topology Optimization
θ	=	Kriging fit hyperparameter
λ	=	Kriging regression hyperparameter

II. Introduction

MACHINE-ASSISTED structures fit a new class of structural optimization, where design initial conditions (ICs), boundary conditions (BCs), and design features are inputted into a machine learning (ML) model to

[1] Student, Department of Aerospace Engineering, AIAA Student Member (ID 1810737), Undergraduate Team.
[2] Student, Department of Aerospace Engineering, AIAA Student Member (ID 1810933), Undergraduate Team.
[3] Student, Department of Aerospace Engineering, AIAA Student Member (ID 1810894), Undergraduate Team.
[4] Student, Department of Aerospace Engineering, AIAA Student Member (ID 1344102), Undergraduate Team.

fulfill a set of requirements. Topology Optimization (TO) and metal additive manufacturing (AM) has been utilized successfully in reducing part mass and massively reducing stress.[5] When applying a ML surrogate to a multi-feature TO simulation, the meta-optimization process results in a "machine-assisted" design, which is up to **6-10x** better than human-created designs, as verified by a study performed by NASA.[5] These structures are designed, optimized, and undergo structural and vibrational testing. In a first for this domain of research, they will be tested in-flight on a student designed rocket.

To reduce the simulation time required by full order modeling, a regressing Kriging surrogate is employed via a MATLAB routine discussed later. In ANSYS, level-set topology optimization can be parameterized so that the weights of the optimizer skew towards either structural compliance, natural frequency, or stress minimization. In practice, static compliance and 1st mode weights control the optimization. In general, topology optimization needs a static structural instance to get stresses, displacements, and strain energy. Then, the optimizer removes material and slightly shifts or deletes nodes every iteration until a mass constraint is met. This process removes material intelligently, while also reducing mass and increasing natural frequency. In the ML approach, multiple simulations are run with a wide range of input features to get a "loss landscape" to minimize.

The Kriging MATLAB surrogate is a k-dimensional regression model that uses scaled, stacked Gaussian functions. The samples are input as $k\,x\,1$ dimensional vectors, and the model generates a scalar output. Interestingly, the model uses covariance between all points and fits hyperparameters—θ and λ—to ensure that the model has a 100% chance of predicting the model X points. Then, the hyperparameters control the level of effect each dimension has on the loss landscape. Figure 1 below shows the process of this model.

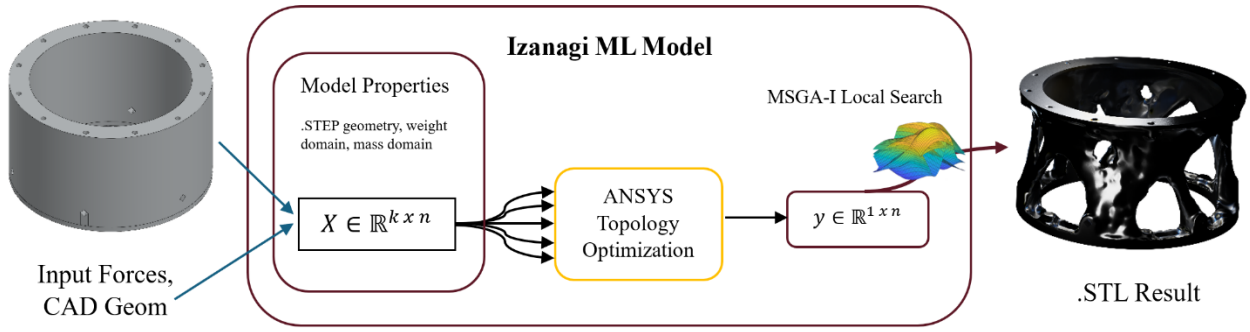

Fig. 1 Aft Truss topology optimization process

This paper focuses on two metal AM + topology optimized parts. First, the Aft Truss is a compressive truss that functionally extends the nozzle on the Helios 2025 Competition Vehicle to the end of the boattail. It is 5" outer diameter, 2.80" height, hollow, and allows for fastener tensioning on the forward and aft end. Its only role is to handle compression. Second, the Lazarus Hybrid Avionics Coupler (HAC) is a multifunctional part that holds avionics, an airbrake mechanism, resists bending, and serves as a central detachment point for the Helios vehicle. Due to a lab electrical failure, this part will be added as a follow-up later for this paper.

The parts are printed via the Renishaw AM400 Laser Powder Bed metal printer in the Center for Advanced Vehicular Systems (CAVS) AM Lab. All parts are printed in AlSi10Mg, which offers the best price/performance and malleability.

Vibration testing was performed in conjunction with NASA Marshall Space Flight Center (MSFC) ET-40 and ET-73 vibration testing group. Vibration tests verify that the Aft Truss prints can withstand the launch environment and confirm that the computational models of the parts are accurate. To verify structural max limit loads, the Aft Trusses will undergo failure testing at the Advanced Composites Institute (ACI). Due to the same AM Lab electrical issue, this testing will occur later with follow-up in the near future. This will further quantify the factors of safety (F.S.) on the parts and instill confidence in the metal printing process. Finally, after testing, the parts will be installed and integrated into the Helios 2025 Space Cowboys competition vehicle. Following flight tests in March and April 2025, post-flight data will be posted in AIAA.

This paper first details the computational methodology of an AM part designed by humans and ML. Then, the design, computational, and experimental methodology between the human and ML designed "Aft Truss" is explained. Finally, the experimental and computational results are discussed, along with implications for further testing.

III. Computational Methodology

A. GSTOR-1 Test Run

GSTOR-1, or the Generative STructural Optimization Routine, develops topology optimized, AM-printed parts from user-defined feature domains. This model was tested on a simplified geometry of the NASA Excite Bracket Challenge, shown to the right in Fig. 2.

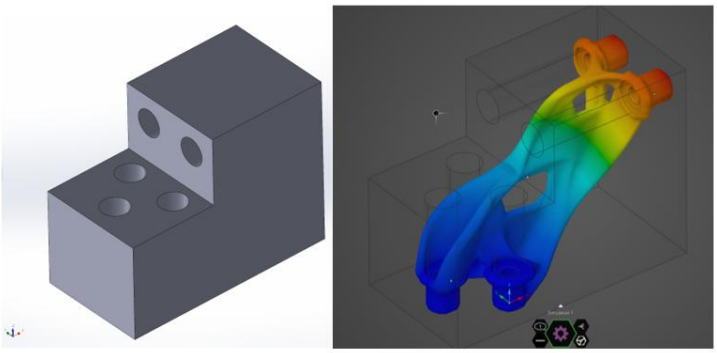

Fig. 2 Bracket before and after topology optimization

First, the parts are constructed in SolidWorks CAD from basic size and interface requirements. Then, the structure is filled in with bulk extrusions, which act as the "generative" region of the routine. There must be care in this process to ensure that interface points are technically feasible. Infeasible regions must be manually cut-extruded from this geometry, which may be a region for improvement in future GSTOR versions.

Next, the geometry is processed with Ansys Mechanical and set up for multiple simulations on the supercomputer clusters at the Mississippi State High Performance Computing Collaboratory (HPCC). After the geometry is set up, the MATLAB routine creates a surrogate with a Random Latin Hypercube (RLH) sampling process. This model then builds a list of batch commands to run on an undergraduate cluster. This cluster has 128 cores/node, and up to four simulations are run at once on one node. The batch scripts then execute the Ansys sample runs, with each run containing a different mass % retainment and objective weight vector. As the designs finish, the results are fed back into the model to form the Kriging regression prediction, after being processed by a cost function. Because every design has different stresses and mass, a scalarization or cost function is used to standardize the performance and isolate the best design. The cost or loss function for GSTOR-1 is shown below in Eq. 1:

$$\mathcal{L} = \sum_{i=1}^{N} \lambda_i \sigma_{norm} + \sum penalty$$
$$\boldsymbol{\theta}, \lambda = \underset{\boldsymbol{\theta},\lambda}{\operatorname{argmin}}\, \mathcal{L}(\boldsymbol{\theta}, \lambda) \tag{1}$$

Where $\mathcal{L}$ is the loss function, λ_i is the i-th weight vector, σ_{norm} is the normalized max stress of the i-th FEA, and the penalty is the mass and build failure soft constraint. The minimum of the loss function is the design with the least stress and minimal mass and build penalty. An internally developed genetic algorithm, MSGA-I, searches the loss landscape for the best design, and then the final design is presented to the user. From a test run of GSTOR-1, shown below in Figure 3, the best design is usually a combination of multiple objectives on a convex loss landscape. This behavior is predictable for low dimensionality (<10 DoFs). After the success of the test run, proven by high accuracy in the ML metrics (0.1734 normalized Root Mean Square Error), real flight hardware was pre-designed and processed.

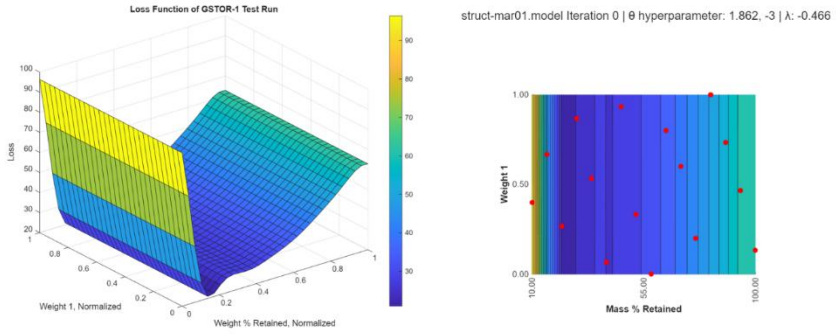

Fig. 3 GSTOR-1 test run ML loss function model, 3D and tileplot view

To get the input forces to the static structural instances, the worst-case flight conditions are exerted on the parts and forces are solved analytically. For aerodynamic forces on some part surfaces, CFD runs are executed to extract the worst-case aerodynamic loading. The CFD pressure distributions are out-of-scope for this paper; a RANS CFD run was performed with Flowpsi using a turbulent model, shown below in Fig. 4.

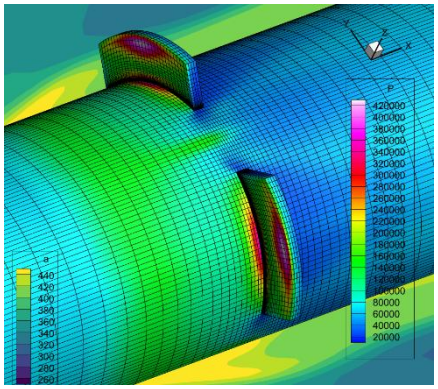

Fig. 4 CFD worst-case loads

B. Aft Truss Design

The aft-truss structure was designed to extend the nozzle of the Aerotech O5500X solid rocket motor to the end of the Helios flight vehicle tail cone. As such, the structure needs to transfer the overall thrust load to the rocket airframe, which is mostly compression.

Two trusses were designed, tested, and compared. First, the "engineered" truss is the truss designed by a human designer using DFAM (design-for-AM) rules. This truss weighs 0.75 lbs when printed. Then, the "machine-assisted," or truss designed by GSTOR-1, was printed alongside its human brethren. It weighs even less, at 0.62 lbs. GSTOR-1 was configured to handle mostly compression, with off-loading in the shear directions (X, Y). Then, GSTOR-1 solved for the most optimal design. Both versions of the Aft Truss are compared below, in Fig. 5.

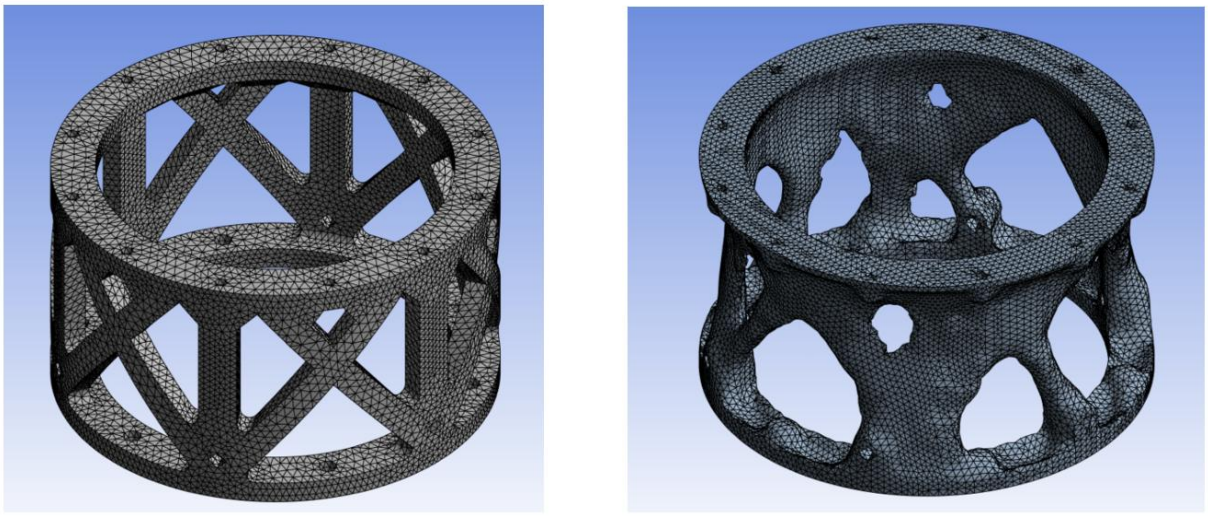

Fig. 5 Engineered (left) and topology optimized (right) truss mesh

C. Vibrational

Vibrational pre-analysis was performed using Ansys in free-free and fixed test conditions. Performing the free-free modal analysis is simple. The parts are individually meshed, materials configured and then solved using the

PCG-Lanczos iterative algorithm. Since the 1st natural frequency was not a huge concern for this part, GSTOR-1 was not configured to optimize the 1st rigid body mode. If the user desired, GSTOR-1 could be configured to satisfy a natural frequency constraint.

D. Structural

Utilizing the Ansys Static Structural analysis system, the engineered and machine-assisted part CAD geometries were loaded for compressive failure prediction. The parts were meshed with a 1mm element size, with the machine-assisted part requiring the Layered Tetrahedrons method. A force vector of 2000 pounds of compression was applied to the top surface. Fixed support definitions were applied on the bottom surface of the model to define the fixed boundary conditions under compressive testing. The model solution was programmed to solve the total deformations and Equivalent (von-Mises) stresses. To find the yield stress, the input load was gradually incremented until the Von-Mises stress exceeded 270 MPa in either part. This stress is the yield stress of AlSi10Mg as provided by an online vendor.[2]

IV. Experimental Methodology

A. Vibration Testing

The engineered Aft Truss as well as the machine-assisted Aft Truss were vibration tested at NASA Marshall Space Flight Center (MSFC) with the assistance of the ET-40 and ET-73 groups. Parts were tested with the T2000 electrodynamic shaker family. Two tests were conducted for each truss in each axis, with a pre-random sine sweep followed by a random vibration test. Thus, 12 tests were performed in total. The T2000H actuates horizontally, which tests the X and Y axes. The other shaker performs vertical actuation for testing in the Z axis. The initial sine-sweeps collected frequency-dependent response data, including natural frequencies that will be activated during the random vibe.[8] The random tests were used to simulate the launch environment and stress the parts at all frequencies simultaneously.[9]

The parts were tested in the 20-2000 Hz frequency range, which is standard practice for aerospace components, as any frequency above that range is unlikely to occur during launch.[6] For the sine-sweeps, the maximum g level was set to 0.25 g, which is slightly higher than the typical test level of 0.1 g.[7] This is because the test type used was development testing, a method that allows for identification of potential issues during the design phase. The sweep rate for sine testing was 2 octaves per minute, which was slow enough to allow accurate data collection, but fast enough that the trusses would not linger at any damaging frequencies for too long.

The random vibration tests followed the General Environmental Verification Standard (GEVS).[4] It provides acceleration spectral density (ASD) levels for different frequency ranges within the overall range, as well as the tolerance and maximum gRMS. This table is used for components weighing 22.7 kg or less. The aft trusses weigh less than 1 kg, fitting them well within the threshold for these levels. The test duration was one minute for each axis.

Table 1. Generalized Random Vibration Test Levels for ELV Components (22.7 kg or less)

Frequency (Hz)	ASD Level (g^2 / Hz)
20	0.026
20-50	+ 6 dB / oct
50-800	0.16
800-2000	- 6 dB / oct
2000	0.026
Overall gRMS: 14.1 (Tolerance: +/- 3 dB)	

A test fixture for the trusses was produced in-house by members of the MSU Space Cowboys. The fixture was designed such that it could also be used for other test articles as well as the trusses. Results were obtained from a tri-axial response accelerometer, which was placed on the top ring for each truss. Additionally, two tri-axial accelerometers were placed on the fixture itself as controls, as shown in Fig. 6. For the sine sweeps, plots of acceleration versus frequency were recorded. For the random tests, plots of ASD versus frequency were recorded.

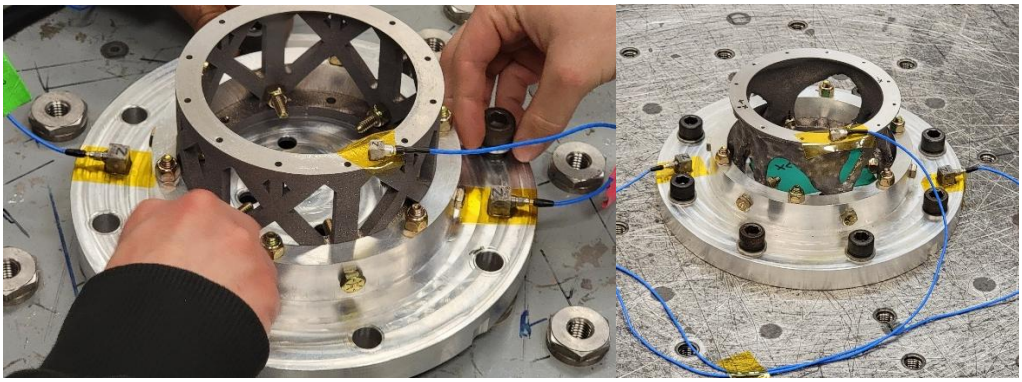

Fig 6. Vibration test configuration for engineered (left) and topology optimized (right) trusses

B. Structural

The physical investigation of the compressive behaviors on both the engineered and topology optimized aft trusses will be tested at the Advanced Composite Institute (ACI) in Starkville, MS using the Universal Testing Machine (UTM) shown in Fig. 7. The test follows ASTM E9 testing specifications. Initially, the specimens' weight and dimensions are confirmed and then visually inspected for faults and defects in manufacturing. Both trusses will be placed on a cylindrical test plate and loaded in the UTM loading space in two separate runs. Axial loading will be applied on the structures until structural fracture or buckling, detected by the UTM. The yielding compressive strength, ultimate compressive strength, and deformation will be recorded in both for each individual trusses.

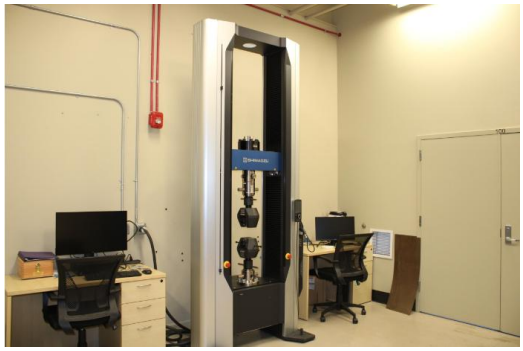

Fig. 7 Universal Testing Machine at MSU ACI

C. Flight Testing

The Aft Truss and HAC will be integrated into the Helios competition vehicle after verification of computational and experimental methodologies. The initial flight test will be conducted prior to the Spaceport America Cup competition for the purpose of validating flight-performance of the vehicle. This flight will provide a boost-phase and coast phase to provide dynamic-loading conditions with accelerations of up to 25 g. The parts will be visually inspected for physical damage post-flight to ensure that they can be reused for future flights.

V. Computational Results

A. Vibrational

The free-free 1st rigid body modes of both trusses are shown in Fig. 6. Table 1 on the next page numerically compares the two.

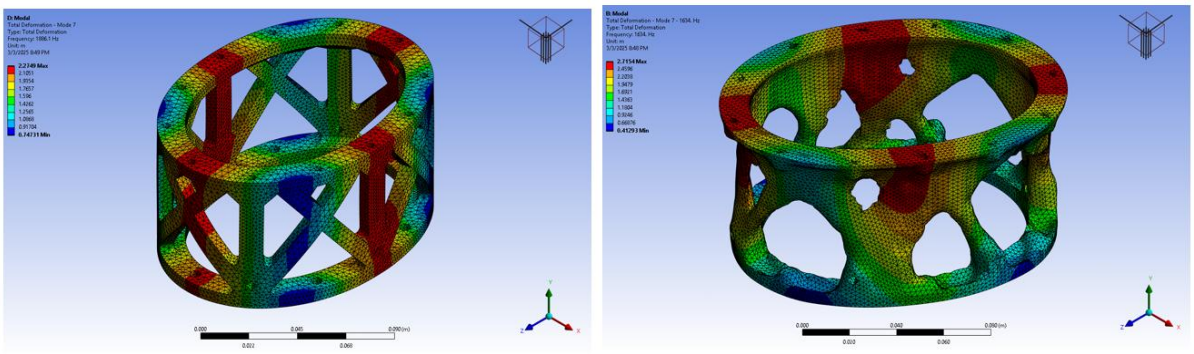

Fig. 8 Engineered (left) and optimized (right) vibrational response

Table 2. Vibratory properties comparison between engineered and machine-assisted trusses

Metric	Engineered Aft Truss	Machine-Assisted Aft Truss
1st Mode	1886.1 **Hz**	1634 **Hz**
Specific 1st Mode	5544 **Hz/kg**	5812.9 **Hz/kg**

B. Structural

Below, Fig. 9 compares the performance of the trusses at 43.0 kN and 52.0 kN. Table 3 highlights the increase performance of the optimized truss in yielding stress predicted in the FEA.

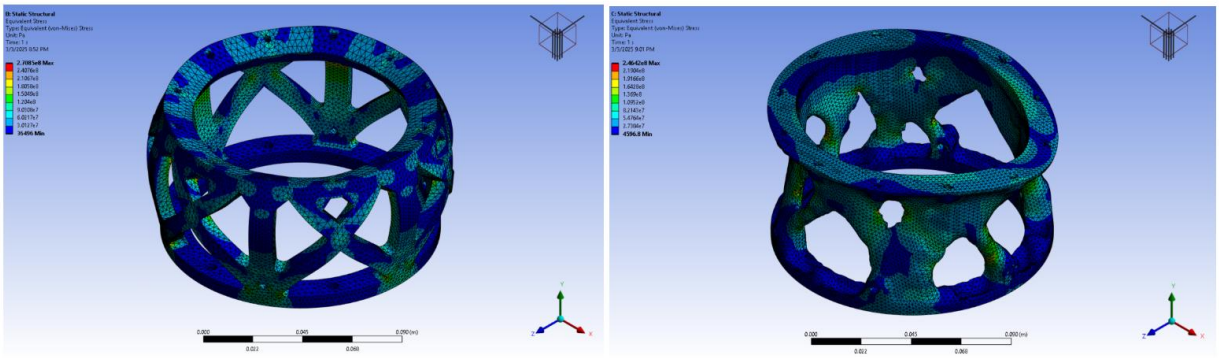

Fig. 9 Engineered (left) and topology optimized (right) truss structural FEA

Table 3. Structural comparison between engineered and machine-assisted trusses

Metric	Engineered Aft Truss	Machine-Assisted Aft Truss
Yield Stress	43.0 **kN**	52.0 **kN**
Specific Yield Stress	126.4 **kN/kg**	185.0 **kN/kg**

VI. Experimental Results

A. Vibration Tests

For the x-axis sine sweeps, the acceleration responses are generally the same for each truss up to the very end of the frequency range, where the topology optimized truss reaches a slightly higher acceleration than that of the engineered truss. In the x-axis random test plots, the response between the two trusses is similar until the end of the frequency range is reached, at which point the ASD response from the topology optimized truss is slightly higher

than that of the engineered truss. Since these components are symmetrical, a similar response difference can be seen in the sine and random Y-axis plots as well. The Z-axis sine and random plots follow the same trend, with higher response values for the topology optimized truss towards the end of the frequency range.

In the following figures, the acceleration profiles for each test are displayed. The response plots for the engineered truss are on the left, while the plots for the topology optimized truss are on the right. Pink represents the X-axis, green represents the Y-axis, and blue represents the Z-axis. For the sine sweeps, acceleration in g's is plotted against frequency in Hz. For the random tests, ASD in g^2/Hz is plotted against frequency in Hz.

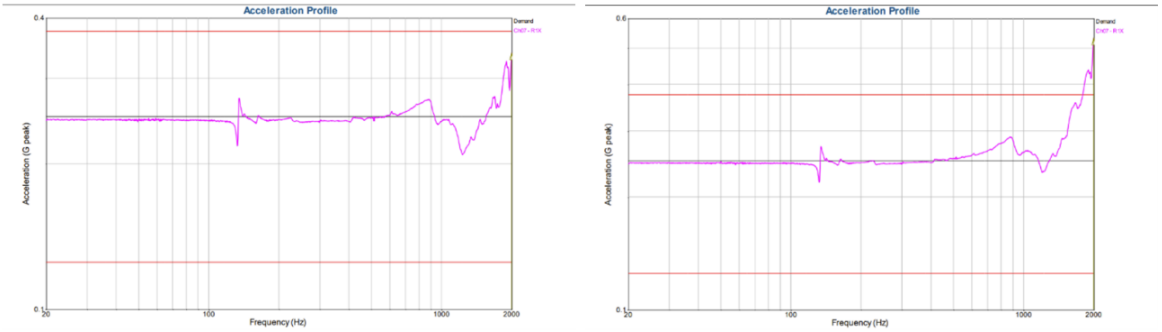

Fig. 110 Engineered (left) and topology optimized (right) truss sine-sweep response (X-Axis)

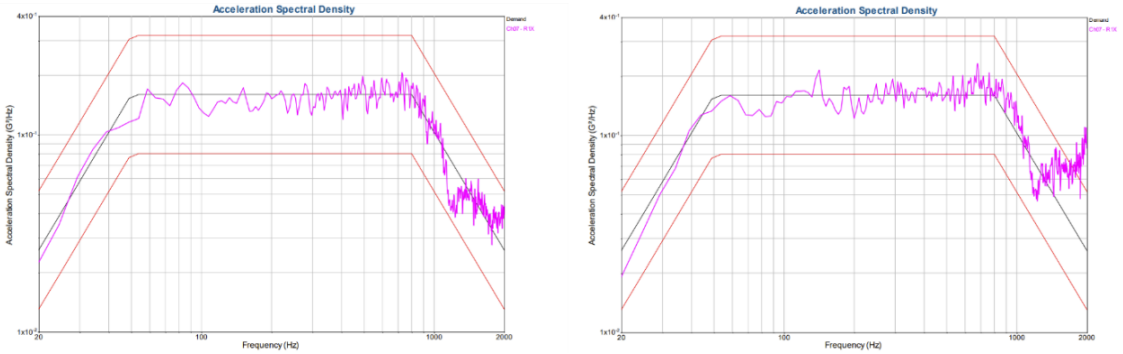

Fig. 11 Engineered (left) and topology optimized (right) truss random vibration response (X-Axis)

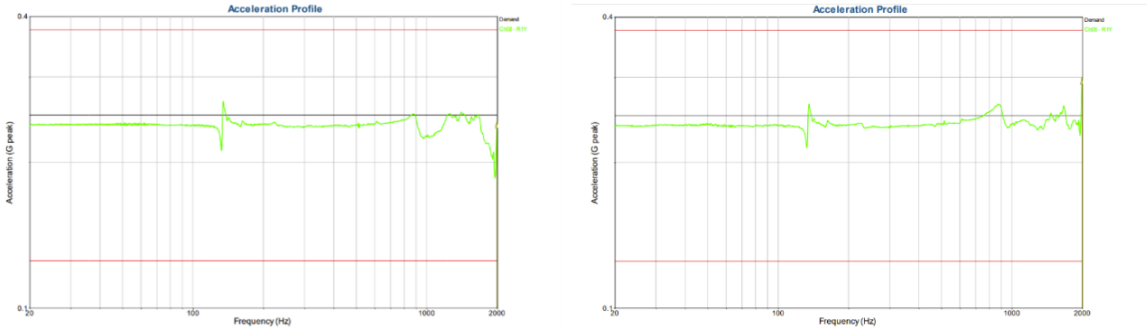

Fig. 12 Engineered (left) and topology optimized (right) truss sine-sweep response (Y-Axis)

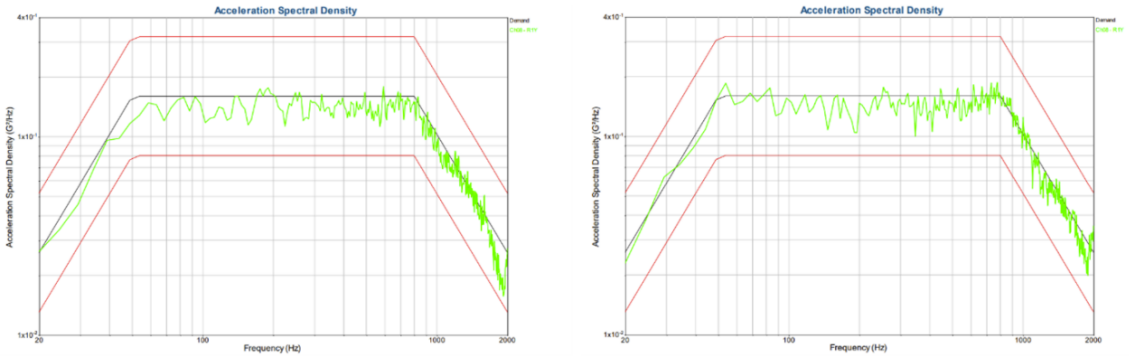

Fig. 13 Engineered (left) and topology optimized (right) truss random vibration response (Y-Axis)

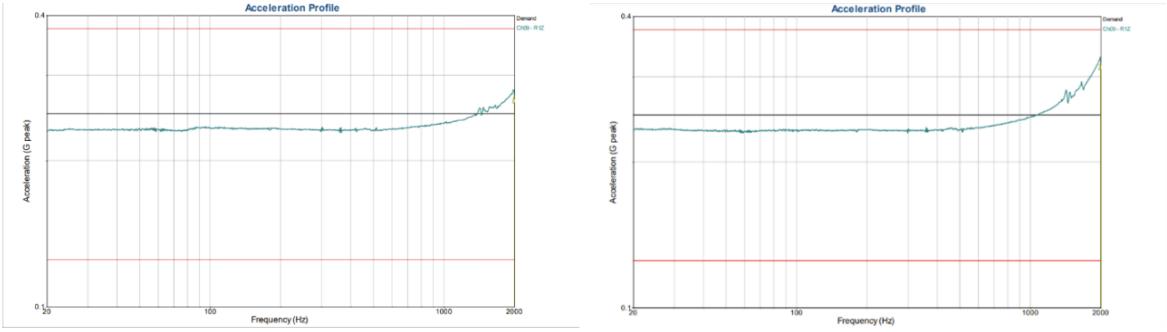

Fig. 14 Engineered (left) and topology optimized (right) truss sine-sweep response (Z-Axis)

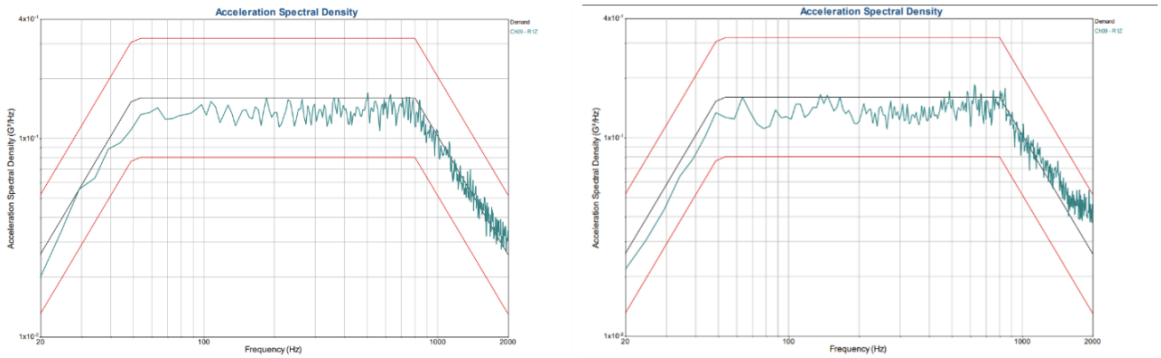

Fig. 15 Engineered (left) and topology optimized (right) truss random vibration response (Z-Axis)

VII. Discussion

A. Vibrational Performance

In the computational results, the engineered truss reaches its first free-free mode at a frequency roughly 200 Hz greater than that of the topology optimized truss. This observation indicates that the engineered truss will perform slightly better than the topology optimized truss. Furthermore, as shown in Table 2, the machine-assisted truss has a specific first mode 5% greater than the engineered truss. GSTOR-1, even without directly programming to focus on natural frequency, outperforms human designs.

Overall, it can be observed that no significant modes are displayed on any of the vibration testing plots (Fig. 10-15), indicating that either truss can easily withstand the vibration sustained in the launch environment. However, there are subtle differences in the acceleration level as well as ASD as the trusses approach higher frequencies. These discrepancies are very small, which indicates that the engineered truss and topology optimized truss will perform about the same during launch, at least from a vibration standpoint. However, since both trusses had no notable modes below 2 kHz, and the topology optimized truss is lighter, it is evident that this truss has superior mass-specific performance.

B. Structural Performance

In simulation, the machine-assisted Aft Truss outperforms the engineered Aft Truss. Table 3 shows that the machine-assisted truss is 21% better in raw yield stress, and 46% better in specific yield. Based on simulation alone, GSTOR-1 defeats a human engineer; later real-world tests will determine if these simulations are indicative of reality.

C. Flight Testing – Aft Truss

The first test-launch of the Space Cowboys competition vehicle is expected to occur no later than March 25, 2025. The Aft Truss and HAC are expected to withstand the flight conditions of the launch environment and be reusable. If the part is found to have physical damage post-flight, a re-evaluation of the methodology will be conducted. If the Aft Trus and HAC are observed to be in flight ready conditions, these parts will continue to be used for the Spaceport America cup competition.

VIII. Conclusion

Technological advances as much as fractions of a percent are praised in the aerospace domain. ML models and machine-assisted structures prove that even with hundreds of years of engineering, near-OOM improvements in design are still possible. Even if those designs are only realized in simulation for complex parts, the fact that ML can beat humans in contemporary design is extraordinary. Thus, topology optimized ML structures provide the structural breakthrough that could lead to another revolution in manufacturing. As the price of additively manufactured components continues to decrease, and applications of space-based manufacturing are explored, the authors suggest further exploration of the domain. Future research in this direction should focus on validating structural FEA results through destructive physical testing using the UTM. Additionally, more parts will be manufactured, with more input features fed into GSTOR. It is the hope that a larger meta-optimization model, or even an internal improvement to TO solvers, will allow for even more improvement.

Appendix

Additional RANS Simulation CFD Grid

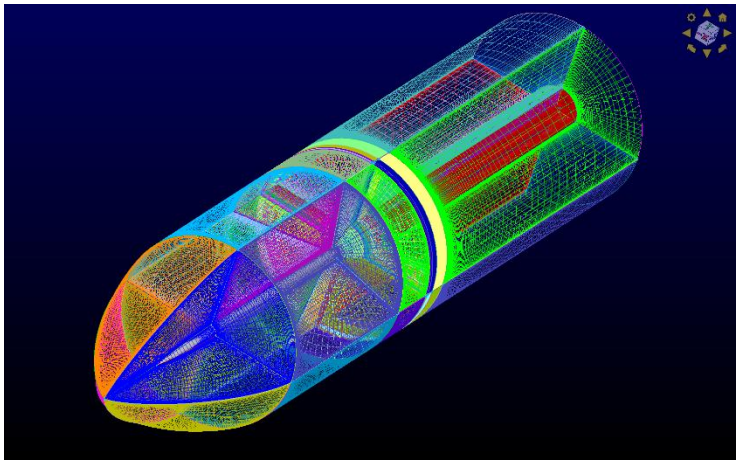

Acknowledgments

We would like to thank Dr. Eric Collins, Dr. Shreyas Narsipur, and Mr. Rob Wolz for their mentorship on this project. Additionally, we would like to thank the Mississippi State HPCC, CAVS, ACI, and ET-40/ET-73 at NASA MSFC for their support and testing resources.

References

[1] *Standard test methods of compression testing of metallic materials at room temperature. E9. (n.d.).* https://www.astm.org/e0009-19.html
[2] EOS GmbH Electro Optical Systems, *"Material Datasheet EOS Aluminium AlSi10Mg,"* EOS e-Manufacturing Solutions, Rev. 04, April 2020, https://www.eos.info/var/assets/03_system-related-assets/material-related-contents/metal-materials-and-examples/metal-material-datasheet/aluminium/material_datasheet_eos_aluminium-alsi10mg_en_web.pdf
[3] Michel, Silvain A., Rolf Kieselbach, and Hans Jörg Martens. *"Fatigue strength of carbon fibre composites up to the gigacycle regime (gigacycle-composites)."* International Journal of Fatigue 28.3 (2006): 261-270.
[4] *General Environmental Verification Standard (GEVS) for GSFC Flight Programs and Projects*.
[5] NASA Goddard, *"Generative Design and Digital Manufacturing: Using AI and Robots to Build Lightweight Instruments,"* NASA Goddard Space Flight Center, https://ntrs.nasa.gov/api/citations/20220012523/downloads/McClelland-Generative%20Design%20SPIE%202022.pdf
[6] Sarafin, T, Doukas, P, Demchak, L, and Browning, M. *"Part 1: Introduction to Vibration Testing*," Vibration Testing of Small Satellites. Instar Engineering and Consulting, Jul. 2017.
[7] Sarafin, T, Doukas, P, Demchak, L, and Browning, M. *"Part 2: Test Configuration, Fixtures, and Instrumentation,"* Vibration Testing of Small Satellites. Instar Engineering and Consulting, Jul. 2017.
[8] Sarafin, T, Doukas, P, Demchak, L, and Browning, M. *"Part 3: Low-Level Sine-Sweep Testing,"* Vibration Testing of Small Satellites. Instar Engineering and Consulting, Jul. 2017.
[9] Sarafin, T, Doukas, P, Demchak, L, and Browning, M. *"Part 5: Random Vibration Testing,"* Vibration Testing of Small Satellites. Instar Engineering and Consulting, Jul. 2017.
[10] Zhu, J., et. al. *"A review of topology optimization for additive manufacturing: Status and challenges,"* Chinese Journal of Aeronautics, Vol. 34, No.1, 2021, pp. 91-110. https://www.sciencedirect.com/science/article/pii/S1000936120304520